

Time evolution of an ion-ion plasma after the application of a direct current bias voltage

Vikas Midha,^{a)} Badri Ramamurthi, and Demetre J. Economou^{b)}
*Plasma Processing Laboratory, Department of Chemical Engineering, University of Houston,
Houston, Texas 77204-4004*

(Received 4 October 2001; accepted for publication 18 February 2002)

A one-dimensional fluid model was developed to investigate the time evolution of a positive ion-negative ion (ion-ion) plasma after the application of a direct current (dc) bias voltage. The ion mass and momentum continuity equations were coupled to the Poisson equation for the electric field. The applied bias is shielded and space charge sheaths are formed within the time scale of ion response (ion plasma frequency). When the ion collision frequency is low compared to the ion plasma frequency, electric field oscillations develop in the bulk due to the ion inertia (overshoot). The net charge density in the sheath, the sheath electric field, and the flux and energy of ions bombarding the electrodes all go through maximum values at a time comparable to the ion plasma frequency. Over long time scales the sheaths are in quasiequilibrium with the bulk plasma. At this time, the ion flux on each electrode is twice the free diffusion flux. © 2002 American Institute of Physics. [DOI: 10.1063/1.1468256]

I. INTRODUCTION

Ion-ion plasmas consist of positive and negative ions only (electron-free plasmas). In practice, a small number of electrons can coexist, provided that the dominant negative charge carriers are negative ions; see Ref. 1 for quantification. Ion-ion plasmas can form in the afterglow of electronegative gases,^{2–6} or in the active glow of strongly electronegative gases at relatively high pressures.⁷ In the latter case, the plasma can be stratified in an electronegative core (with a relatively small number of electrons) and an electropositive edge (without negative ions). The transition between the two regions can be smooth, or double layers may separate the two regions.^{8–11} Ion-ion plasmas are important in negative ion sources,¹² the *D* layer of the atmosphere,¹³ in dusty plasmas,¹⁴ and in materials processing.^{15–17}

The electrostatic fields in an ion-ion plasma are determined by ions instead of electrons. The reason for the existence of electrostatic fields in conventional electron-ion plasmas is to balance wall losses of the lighter and more energetic electrons out of the plasma with those of the heavier and colder positive ions. By replacing electrons with negative ions in the plasma, the mass and temperature of the negatively charged and positively charged species become comparable. Ion-ion plasmas, therefore, are characterized by much weaker electrostatic fields, with a plasma potential of the order of the ion temperature (without external bias). In the ideal case of a positive ion-negative ion plasma in which both ion species have equal masses and temperatures, ion-ion plasmas are characterized by the absence of electrostatic fields and the absence of sheaths (when no bias voltage is applied). The spatial profiles of positive and negative ions

coincide throughout the length of the reactor, and both ions are able to diffuse freely to the walls. Other salient features of ion-ion plasmas include^{14,18} (a) only heavy particles participate in plasma chemistry, (b) the plasma impedance can be changed drastically by light irradiation (negative ion photodetachment) that creates electrons, (c) the potential distribution in an ion-ion plasma (without a bias or with a low frequency bias) behaves as in liquid electrolytes,¹⁹ and (d) ion-ion plasma properties can be measured by a Langmuir probe.²⁰

As mentioned above, an ideal ion-ion plasma (ions of equal masses and temperatures) without an external bias potential is characterized by the absence of electrostatic fields and free diffusion of ions to the walls. The profile of positive ion density simply overlaps with the negative ion density. In the presence of a bias potential, however, the positive and negative ions separate to form ion sheaths near the electrode. In this article, the influence of an external direct current (dc) bias on an ion-ion plasma is examined. A time-dependent one-dimensional fluid model of an ion-ion plasma is developed which resolves the sheath region near the electrodes. The model includes the Poisson equation for the electrostatic field coupled with the continuity and momentum equations for the ion densities and velocities, respectively. Sheath formation during the initial transient after the application of a dc bias is examined. The rf case was treated in Ref. 21. The transient response of a conventional electron-ion plasma to an applied dc bias has been studied before in connection with plasma immersion ion implantation.^{22,23} The application of a dc bias in the afterglow of a rf plasma was reported by Overzet *et al.*²⁴

II. MODEL DEVELOPMENT

A low-pressure ion-ion plasma formed in the late afterglow of a pulsed chlorine discharge is considered. A high

^{a)}Currently with General Electric-CRD, Schenectady, NY 12065.

^{b)}Author to whom all correspondence should be addressed; electronic mail: economou@uh.edu

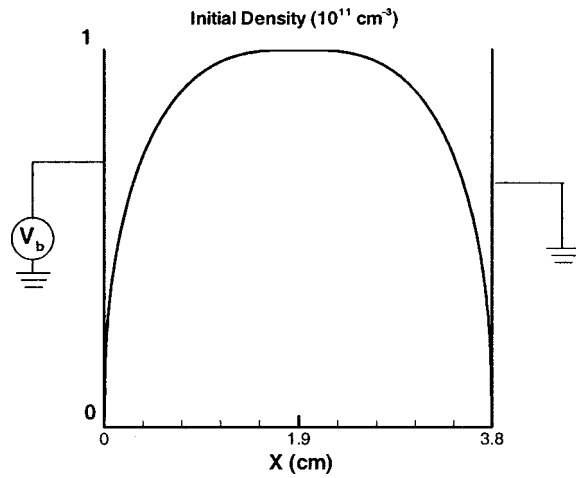


FIG. 1. Schematic of the one-dimensional parallel plate plasma system considered. The initial ion density profile is shown (overlapping positive and negative ion densities). A negative dc bias is applied to the left electrode at time $t=0$. The right electrode is kept at ground potential at all times.

degree of gas dissociation is assumed, making Cl^+ and Cl^- the only ions present. (It should be noted that, in the presence of undissociated gas, charge exchange between Cl^+ and Cl_2 can generate Cl_2^+ ions.²⁵) The electron density is assumed to have decayed to low enough values compared to the ion density (electronegativity greater than ~ 1000), so that the presence of electrons may be completely neglected. Similarly, any electrons that may be generated due to the applied bias are neglected.⁴ The parallel electrodes are assumed to be of equal area (one-dimensional system). A negative dc bias voltage is applied to the driven (left) electrode, while the other (right) electrode is grounded (Fig. 1).

A one-dimensional time-dependent fluid model of the ion-ion plasma under the influence of an externally applied bias potential is developed. The model consists of the following set of governing equations.

The continuity equation for the positive and negative ions is given by

$$\frac{\partial n_i}{\partial t} = -\frac{\partial}{\partial x}(n_i u_i) + R_i, \quad (1)$$

where n_i is the ion density, u_i is the ion fluid velocity, and R_i represents the rate of generation or loss of ions through chemical reaction (ion-ion recombination in this case); $i=p$ and $i=n$ for positive and negative ions, respectively. The ion fluid velocities are computed by the momentum balance equations

$$\frac{\partial(n_i u_i)}{\partial t} + \frac{\partial(n_i u_i u_i)}{\partial x} = \left(\frac{s_i q}{M_i}\right) n_i E - \left(\frac{k T_i}{M_i}\right) \frac{\partial n_i}{\partial x} - n_i u_i \nu_i, \quad (2)$$

where M_i is the ion mass, T_i is the ion temperature, ν_i is the ion-neutral collision frequency, s_i is the charge number of the ion, and q is the value of the elementary charge. The terms in Eq. (2) (from left to right) represent the time rate of change in ion momentum or temporal inertia, spatial inertia,

TABLE I. Base case parameter values used in the simulation.

Initial peak ion density	10^{11} cm^{-3}
Interelectrode gap	3.8 cm
Ion temperature	0.026 eV
Ion mass	35.5 amu
Gas pressure	20 mTorr
Gas temperature	300 K
dc bias potential	-130 V
Reference collision frequency	300 kHz
Ion plasma frequency at the sheath edge	$\sim 30 \text{ MHz}$

electrostatic force, pressure gradient, and collisional drag, respectively. The electrostatic field is governed by the Poisson equation

$$\frac{\partial E}{\partial x} = \frac{q}{\epsilon_0}(n_p - n_n), \quad (3)$$

where the electric field E is related to the plasma potential V by $E = -\partial V/\partial x$. Here ϵ_0 is the permittivity of free space. The potential at the driven (left, $x=0$) electrode is assumed to be $V = -V_b$, a negative dc bias. The potential at the grounded (right, $x=3.8$ cm) electrode is fixed at zero (Fig. 1). A variable collision frequency model (constant mean free path) was used whereby, $\nu_i(u_i) = \nu_{i0}|u_i|/c_s$. Here, $|u_i|$ is the absolute value of the ion fluid velocity u_i , and ν_{i0} is a “reference” collision frequency corresponding to an ion fluid velocity equal to $c_s = \sqrt{kT_i/M_i}$, the ion acoustic speed. For the base case conditions of Table I, the reference collision frequency was taken as 300 kHz. Under the base case conditions the ion mean free path is ~ 1 mm.

The governing equations of the fluid model, therefore, consist of two continuity equations for ion densities n_p and n_n , two momentum equations for ion velocities u_p and u_n , and the Poisson equation for the electrostatic field. Initial conditions were identical positive and negative ion density profiles as obtained in an ion-ion plasma with equal mass and temperature of the ions (nearly parabolic profile if ion-ion recombination is slow, see Fig. 1) with a peak ion density of 10^{11} cm^{-3} , and potential equal to zero everywhere. Boundary conditions included zero positive and negative ion density on the walls. The positive ion/negative ion recombination rate coefficient was taken as $5 \times 10^{-8} \text{ cm}^3/\text{s}$.²¹

III. METHOD OF SOLUTION

The governing system of Eqs. (1)–(3) was discretized in space using a finite-difference scheme based on a staggered mesh.²⁶ Ion densities and plasma potential were evaluated on one set of grid points while other dependent quantities (including ion velocities, fluxes, and electric field) were evaluated on a staggered set of grid points. Upwind-biased finite-difference operators were employed to approximate the spatial inertia terms in the ion momentum equations. Discretization in space converted the original set of Eqs. (1)–(3) into a time-dependent differential-algebraic equation (DAE) system. This set of DAEs was solved using LSODI, a fully implicit, variable order, variable time step integrator based on backward difference formulas.²⁷ A nonuniform mesh of 301 grid points biased towards the sheaths near the electrodes was employed.

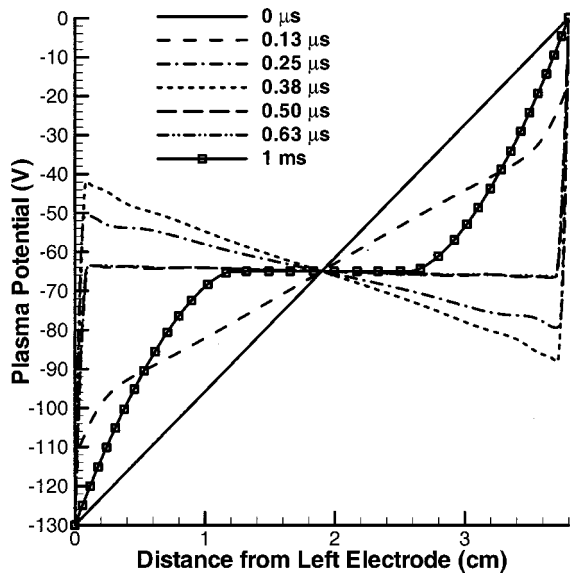


FIG. 2. Time evolution of the potential between the two electrodes for the base case conditions (Table I).

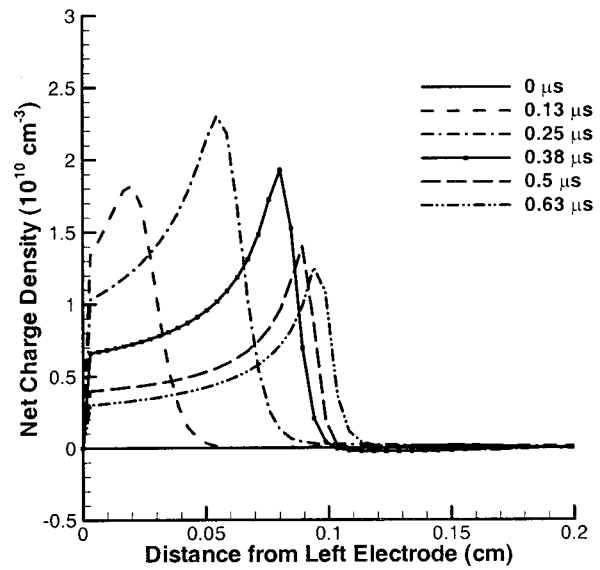


FIG. 4. Time evolution of the net charge density near the left (biased) electrode for the base case conditions (Table I).

IV. RESULTS AND DISCUSSION

An ion-ion plasma formed in the late afterglow of a pulsed chlorine discharge is considered. Initially, the positive and negative ion density profiles overlap (for an ideal ion-ion plasma with equal ion masses and temperatures) with a nearly parabolic profile as shown in Fig. 1. At $t=0$, a negative dc bias is applied to the left electrode, and the evolution of the ion-ion plasma is examined. Figure 2 shows the evolution of the potential along the interelectrode gap, while Fig. 3 shows the evolution of the electric field at the left electrode and at the center of the plasma. Figure 4 shows the net charge density in the region near the left electrode. Figures 5 and 6 show the ion flux and ion energy evolution at the left electrode. All results refer to the base case conditions (Table I), unless noted otherwise.

The initial potential profile is linear (Fig. 2, $t=0$) and a uniform electric field exists along the length of the gap. This electric field attracts positive ions towards the left electrode and negative ions towards the right electrode. Due to ion inertia, however, a finite time is required for ions to respond to the applied electric field. For short times ($0 < t \ll 10^{-7}$ s), therefore, the electric field remains essentially unchanged (Fig. 3) and the ion velocities increase linearly with time due to the applied electric field.

For time scales of the order of 10^{-7} s (a time scale comparable to the ion plasma frequency), there is significant change in the ion density profiles due to acceleration of the ions. At this point in time the applied bias starts to be shielded by the ion-ion plasma due to the formation of sheaths at the electrodes (Fig. 2). Negative ions are repelled from the left electrode while positive ions are attracted. This

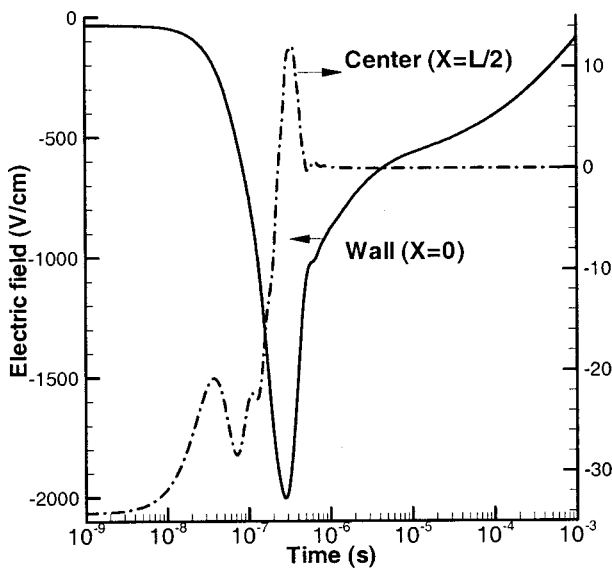


FIG. 3. Time evolution of the electric field at the center (right axis) and at the left (biased) electrode (left axis) for the base case conditions (Table I).

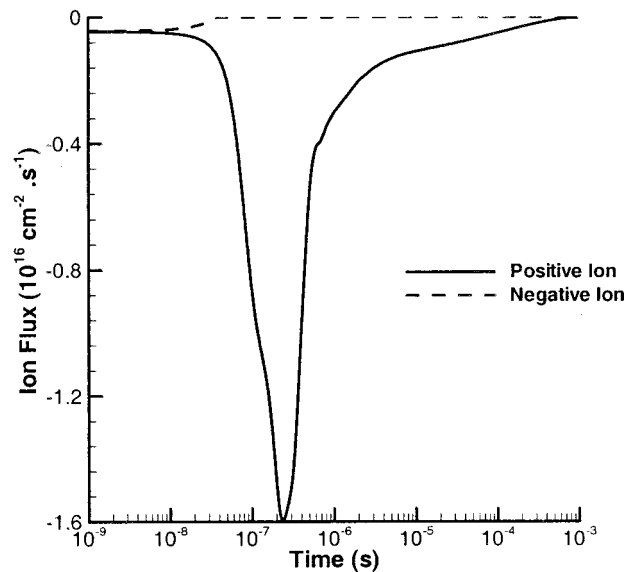


FIG. 5. Time evolution of the positive ion flux on the left (biased) electrode for the base case conditions (Table I).

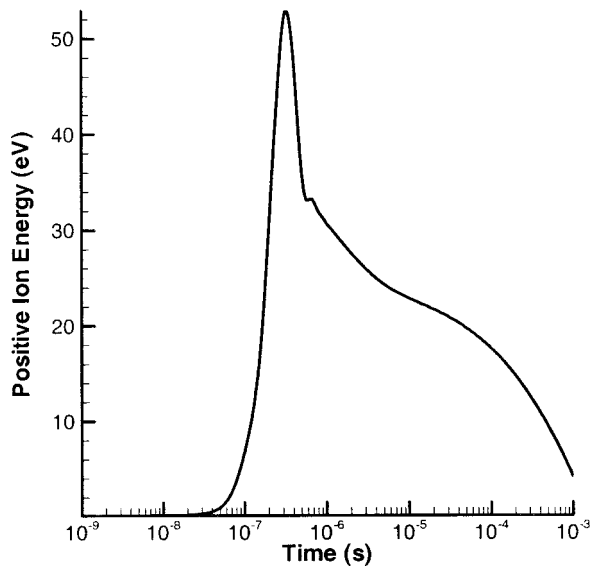


FIG. 6. Time evolution of the positive ion energy on the left (biased) electrode for the base case conditions (Table I).

results in accumulation of net positive charge at the left electrode (Fig. 4). Similarly, negative ions are attracted to the right electrode while positive ions are repelled. Due to the assumed equal masses and temperatures of the positive and negative ions, an equal negative charge is accumulated at the right electrode (not shown).

As a result of charge accumulation, significant potential gradients appear in the sheath next to the electrode (Fig. 2, $t > 10^{-7}$ s). Therefore, while the magnitude of the electric field decreases in the bulk plasma due to shielding, the electric field increases in the sheath regions (Fig. 3, $10^{-7} < t < 3 \times 10^{-7}$ s). Positive ions in the left sheath are accelerated by the electric field resulting in an increase in the positive ion energy and flux to the left electrode (Figs. 5 and 6, $5 \times 10^{-8} < t < 3 \times 10^{-7}$ s). The negative ion flux at the left electrode drops to zero (Fig. 5) as the negative ions are repelled away from the electrode. Similarly, at the right electrode, the negative ion energy and flux increase with time while the positive ion flux is reduced to zero.

Again, as a result of charge accumulation in the sheaths, the applied bias potential is shielded in the bulk plasma. However, due to ion inertia, net charge continues to accumulate in the sheaths and an electric field with the reverse polarity (overshoot) is established in the bulk plasma (Figs. 2 and 3, $2 \times 10^{-7} < t < 5 \times 10^{-7}$ s). This field now retards positive ions moving towards the left electrode and negative ions moving towards the right electrode. As a result, the flux of positive ions from the bulk plasma to the left sheath is reduced. However, within the left sheath, positive ions continue to be accelerated from the sheath towards the electrode. Due to the decrease in positive ion flux from the bulk plasma to the sheath and the continuous extraction of positive ions (out of the sheath towards the electrode) by the field, the overall positive ion density in the sheath starts dropping as a function of time (Fig. 4, $t > 2.5 \times 10^{-7}$ s). The potential pro-

file at long times (Fig. 2 at $t = 1$ ms) indicates that the sheath thickness increases to nearly 1 cm.

The overall evolution of the net charge density in the sheaths, therefore, shows the formation of a peak (Fig. 4, $t = 2.5 \times 10^{-7}$). The net positive charge in the left sheath initially increases as the negative ions are repelled and then decreases as the positive ions are depleted. Similarly, the net charge in the right sheath increases as the positive ions are repelled and then decreases as the negative ion density drops as a function of time (not shown). Consequently, the electric field in the sheaths also shows the formation of a peak with the charge density and decreases after 3×10^{-7} s (Fig. 3). The positive ion energy and flux at the left electrode peak with the electric field in the sheath and then decrease as a function of time (Figs. 5 and 6). The ion mean free path at 20 mTorr is ~ 1 mm, while the sheath at long times is nearly 1 cm thick (Fig. 2). Hence ions suffer several collisions in the sheath resulting in substantially lower ion energy at long times.

The nonmonotonic behavior (overshoot) of the electric field in the bulk plasma under a dc bias is related to the temporal inertia of ions and occurs because the time scale corresponding to the ion plasma frequency (about 30 MHz for an ion density of 10^{10} cm^{-3} near the sheath edge) is significantly lower than the characteristic collision time reference (collision frequency of 300 kHz at 20 mTorr) at the base conditions examined here (Table I). For time scales longer than this characteristic collision time, oscillations in the electric field are damped in the bulk plasma and ion transport is governed by ion drift and diffusion (the mobility and diffusion coefficients for the ions, however, are not constant but change as the collision frequency varies with ion velocity). In the sheaths, the spatial inertia of the ions [second term on the left-hand side of Eq. (2)] is also important since the mean free path of the ions at this operating pressure (~ 1 mm) is smaller than the sheath thickness.

For time scales longer than the characteristic collision time ($t > 10^{-6}$ s in this case), the charge density in the left sheath decays as a function of time until the positive ion flux from the sheath to the walls is balanced by the positive ion flux from the bulk plasma to the sheath. Concurrently, the sheath edge expands as a function of time, and the negative ion front sharpens until the negative ion drift flux (away from the left electrode) is nearly balanced by the negative-ion diffusion flux (towards the left electrode). Beyond this time scale, the sheath is in quasisteady state with respect to the decaying bulk plasma and the ion flux at the electrode is limited by diffusion (Fig. 5, $10^{-5} < t < 10^{-4}$ s). Hence, eventually, the dc bias simply redistributes the total diffusion flux between the two electrodes; all positive ions exit the left electrode while all negative ions exit the right electrode. The total ion flux at each electrode is limited by twice the diffusion flux of ions, as in the case of liquid electrolytes with equal masses of positive and negative ions.¹⁹ The overall plasma decays on a time scale corresponding to diffusion of ions across the gap and later on by ion-ion recombination (for $t \gg 10^{-4}$ s).

Figures 7(a) and 7(b) show the effect of varying bias voltage on the temporal evolution of the Cl^+ flux on the left

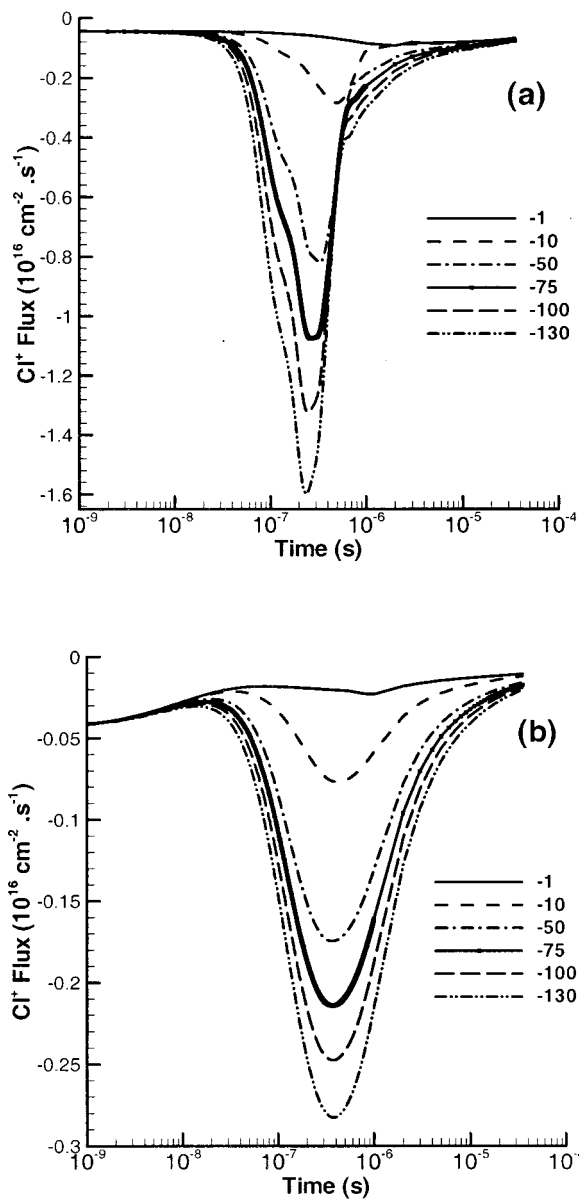


FIG. 7. Time evolution of the positive ion flux on the left (biased) electrode for bias voltages of -1 , -10 , -50 , -100 , and -130 V, and reference collision frequencies of (a) 300 kHz and (b) 30 MHz. Other conditions are as in Table I.

electrode, for reference collision frequencies of 300 kHz and 30 MHz, respectively. As the bias voltage is increased, the velocity of ions through the sheath also increases. This leads to larger spatial inertia, hence an increase in the peak ion flux. The width of the temporal profile is larger in Fig. 7(b), compared to that in Fig. 7(a), due to larger ion collisionality. The position of the peak shifts to smaller times as the bias voltage is increased in Fig. 7(a), gradually approaching a constant temporal position for large bias voltages. This is due to the nonlinearity of the collision term in the momentum equation [Eq. (2)]. For larger bias voltages, the ion fluid velocity is correspondingly higher, the ion collisionality increases, and the temporal location of the peak reaches a constant value. This is consistent with Fig. 7(b), where the peak shift is comparatively much smaller due to already large collision frequency. Also, because of the larger collision fre-

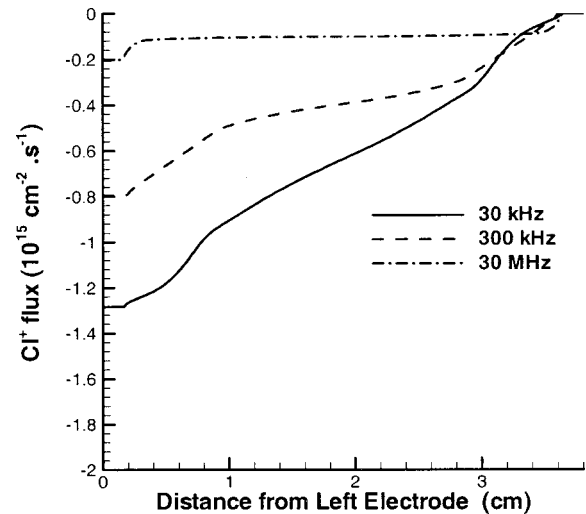


FIG. 8. Spatial dependence of positive ion flux 35 μ s after the application of a dc bias of -130 V, for reference collision frequencies of 30 kHz, 300 kHz, and 30 MHz. Other conditions are as in Table I.

quency, the peak value of the flux is about an order of magnitude smaller.

For practical purposes, one may think of the following scenario. A pulsed chlorine discharge may be employed with a pulse period of 100 μ s and a duty ratio of 0.5 (50 μ s for the active glow and 50 μ s for the afterglow). During each of the afterglow periods, electrons disappear within 15 μ s, leaving behind an ion-ion plasma.¹ A negative bias is then applied to this ion-ion plasma for the remaining 35 μ s of the afterglow. The spatial profile across the gap of the Cl⁺ flux, 35 μ s after the application of the dc bias, is shown in Fig. 8, for three reference frequencies (30 kHz, 300 kHz, and 30 MHz). The bias voltage was held constant at -130 V for all three cases. For a collision frequency (30 MHz) comparable to the ion plasma frequency, ion motion is in a quasisteady state, resulting in a constant flux across the bulk plasma and rapid changes near the walls (in the sheath) only. When the collision frequency (30 kHz) is much smaller than the ion plasma frequency, ion motion is not in a quasisteady state, giving rise to a nonuniform flux in the bulk plasma. An intermediate situation is observed for an intermediate frequency (300 kHz). The ion flux to the electrodes increases considerably as the collision frequency (or pressure) decreases.

IV. CONCLUSIONS

A time-dependent one-dimensional fluid model was developed to investigate the initial response of a positive ion-negative ion (ion-ion) plasma to an applied dc bias. The ion mass and momentum continuity equations were coupled to the Poisson equation for the electric field. The applied bias is shielded and space charge sheaths are formed within the time scale of ion response (ion plasma frequency). Because the ion collision frequency is low compared to the ion plasma frequency, electric field oscillations occur in the bulk due to the ion inertia (overshoot). For time scales longer than the ion collision time, however, these oscillations are damped and ion transport is governed by drift and diffusion. The net

charge density in the sheath, the sheath electric field, and the flux and energy of ions bombarding the electrodes all go through maximum values at a time comparable to the ion plasma frequency. Over longer time scales the sheaths are in quasiequilibrium with the decaying bulk plasma. At this time, the dc bias simply redistributes the total diffusion flux between the two electrodes; all the positive ions exit the left electrode while all the negative ions exit the right electrode. The total ion flux at each electrode is limited by twice the diffusion flux of ions, as in the case of liquid electrolytes with equal masses of the positive and negative ions. The overall plasma decays on a time scale corresponding to diffusion of ions across the length of the reactor and further on by ion-ion recombination (for $t \gg 10^{-4}$ s). As the ion collision frequency increases from 30 kHz to 30 MHz, the peak ion flux drops by an order of magnitude.

ACKNOWLEDGMENTS

The authors are grateful to the National Science Foundation (CTS-9713262 and CTS-0072854) and the State of Texas (Texas Advanced Technology Program) for financial support of this work. Many thanks to Dr. I. D. Kaganovich and Dr. V. Mani for helpful technical discussions.

- ¹V. Midha and D. J. Economou, *Plasma Sources Sci. Technol.* **9**, 256 (2000).
- ²I. Kaganovich, D. J. Economou, B. N. Ramamurthi, and V. Midha, *Phys. Rev. Lett.* **84**, 1918 (2000); I. Kaganovich, B. N. Ramamurthi, and D. J. Economou, *Phys. Rev. E* **64**, 036402 (2001).
- ³A. Smith and L. J. Overzet, *Plasma Sources Sci. Technol.* **8**, 82 (1999).
- ⁴M. V. Malyshev, V. M. Donnelly, J. I. Colonell, and S. Samukawa, *J. Appl. Phys.* **86**, 4813 (1999).
- ⁵S. A. Gutsev, A. A. Kudryavtsev, and V. A. Romanenko, *Tech. Phys.* **40**, 1131 (1995).
- ⁶D. Smith, A. G. Dean, and N. G. Adams, *J. Phys. D: Appl. Phys.* **7**, 1944 (1974).

- ⁷A. J. Lichtenberg, I. G. Kouznetsov, Y. T. Lee, M. A. Lieberman, I. D. Kaganovich, and L. D. Tsendin, *Plasma Sources Sci. Technol.* **6**, 437 (1997); R. N. Franklin and J. Snell, *J. Phys. D: Appl. Phys.* **32**, 1 (1999).
- ⁸V. I. Kolobov and D. J. Economou, *Appl. Phys. Lett.* **72**, 656 (1998).
- ⁹I. G. Kouznetsov, A. J. Lichtenberg, and M. A. Lieberman, *J. Appl. Phys.* **86**, 4142 (1999).
- ¹⁰A. Kono, *J. Phys. D: Appl. Phys.* **32**, 1357 (2000); R. N. Franklin and J. Snell, *ibid.* **33**, 1 (2000).
- ¹¹I. D. Kaganovich and L. D. Tsendin, *Plasma Phys. Rep.* **19**, 645 (1993); L. D. Tsendin, *Sov. Tech. Phys. Lett.* **34**, 11 (1989).
- ¹²M. B. Hopkins and K. N. Mellon, *Phys. Rev. Lett.* **67**, 449 (1991); D. Hayashi and K. Kadota, *J. Appl. Phys.* **83**, 697 (1998).
- ¹³W. Swider, *Ionospheric Modeling* (Birkhauser, Basel, 1988).
- ¹⁴H. Amemiya, in *Dusty and Dirty Plasmas, Noise, and Chaos in Space and in the Laboratory*, edited by H. Kikuchi (Plenum, New York, 1994).
- ¹⁵S. Samukawa and T. Mieno, *Plasma Sources Sci. Technol.* **5**, 132 (1996).
- ¹⁶T. Shibayama, H. Shindo, and Y. Horiike, *Plasma Sources Sci. Technol.* **5**, 254 (1996).
- ¹⁷T. H. Ahn, K. Nakamura, and H. Sugai, *Plasma Sources Sci. Technol.* **5**, 139 (1996).
- ¹⁸W. L. Fite and J. A. Rutherford, *Discuss. Faraday Soc.* **37**, 192 (1964); L. J. Puckett and W. C. Lineberger, *Phys. Rev. A* **1**, 1635 (1970); G. A. Woosley, I. C. Plump, and D. B. Lewis, *J. Phys. D: Appl. Phys.* **6**, 1883 (1973).
- ¹⁹J. Newman, *Electrochemical Systems* (Prentice Hall, Engelwood Cliffs, NJ, 1973).
- ²⁰H. Amemiya, *J. Phys. D: Appl. Phys.* **23**, 999 (1990).
- ²¹V. Midha and D. J. Economou, *J. Appl. Phys.* **90**, 1102 (2001).
- ²²Y. El-Zein, A. Amin, C. Shen, S. Yi, K. E. Lonngren, and T. E. Sheridan, *J. Appl. Phys.* **79**, 3853 (1996); M.-P. Hong and G. A. Emmert, *J. Vac. Sci. Technol. B* **12**, 889 (1994).
- ²³K. U. Riemann and Th. Daube, *J. Appl. Phys.* **86**, 1202 (1999).
- ²⁴L. J. Overzet, Y. Lin, and L. Luo, *J. Appl. Phys.* **72**, 5579 (1992).
- ²⁵S. K. Kanakasabapathy, L. J. Overzet, V. Midha, and D. J. Economou, *Appl. Phys. Lett.* **78**, 22 (2001).
- ²⁶M. A. Barnes, T. J. Cotler, and M. A. Elta, *J. Comp. Phys.* **77**, 53 (1988).
- ²⁷C. Hindmarsh, Lawrence Livermore Lab. Report UCRL-87406 (1982) and UCRL-89311 (1983); A. C. Hindmarsh, in *Scientific Computing*, edited by R. S. Stepleman (IMACS, North Holland, Amsterdam, 1983), p. 55.